Bioorganic Chemistry 111 (2021) 104843

Contents lists available at ScienceDirect

Bioorganic Chemistry

journal homepage: www.elsevier.com/locate/bioorg

New dammarane-type glycosides from *Gynostemma pentaphyllum* and their lipid-lowering activity

Xin Weng [a,1], Yun-Yun Lou [a,b,1], Yun-Shan Wang [a,c], Ya-Ping Huang [a], Jian Zhang [c,*], Zhi-Qi Yin [a,*], Ke Pan [b,*]

[a] Department of TCMs Pharmaceuticals, School of TCM & State Key Laboratory of Natural Medicines, China Pharmaceutical University, Nanjing 210009, PR China
[b] Department of Natural Medicinal Chemistry, School of TCM & State Key Laboratory of Natural Medicines, China Pharmaceutical University, Nanjing 211198, PR China
[c] Laboratory of Translational Medicine, Affiliated Hospital of Integrated Traditional Chinese and Western Medicine, Nanjing University of Chinese Medicine, Nanjing, 210028, PR China

ARTICLE INFO

Keywords:
Gynostemma pentaphyllum
Lipid-lowering
Triterpenoid saponin
PCSK9

ABSTRACT

Gynostemma pentaphyllum (Thunb.) Makino has a long history as food and diary supplement in China. At present, there are some products for hyperlipidemia in the market, including *G. pentaphyllum* tea, healthy wine and healthy food. In order to discover proprotein convertase subtilisin/kexin type 9 (PCSK9) inhibitors, fourteen new triterpenoid saponins named gypenoside LXXXVIII-CI (**1**–**14**) along with six known compounds (**15**–**20**) were isolated from *G. pentaphyllum*. Their structures were elucidated by means of various spectroscopic techniques. Eight isolates were evaluated the inhibitory effect on PCSK9 in HepG2 cells. The results showed that three dammarane-type glycosides (**2**, **3**, **15**) remarkably reduced PCSK9 expression at 10 μM concentration. These findings suggested that *G. pentaphyllum* was worthy of further investigation to find small molecule PCSK9 inhibitors and facilitate their utilization as functional food ingredients.

1. Introduction

Gynostemma pentaphyllum (Thunb.) Makino, called "Southern Ginseng", is a member from the Cucurbitaceae family, which mostly distributed in the southern part of Qinling Mountains and Yangtze River [1,2]. *G. pentaphyllum* was originally eaten as a wild vegetable recorded in a medicinal literature called "Herbs for Famine", which was an edible medicinal herb or a dietary supplement in the folk [2]. Modern pharmacological researches supply plentiful evidences of its anti-inflammatory, anti-tumor, anti-hyperlipidemic ability and its regulatory role of liver function [3]. At present, some commercial products from *G. pentaphyllum* including tea and beverages are available and beneficial for hyperlipidemia [4]. In addition, *G. pentaphyllum* was also used as additives in drinks, beer, bread and noodles [5,6].

Hyperlipidemia is a highlighted risk factor for developing atherosclerosis and cardiovascular disease (CVD), and low-density lipoprotein cholesterol (LDL-C) is recognized as an independent risk factor for CVD [7]. Currently, statins are recommended as first-line drugs to reduce LDL-C and prevent CVD. However, there are limited options for patients with severe hypercholesterolemia who are treated on maximally tolerated statin therapy. Proprotein convertase subtilisin/kexin type 9 (PCSK9) is a pivotal regulator of low-density lipoprotein receptors (LDLRs), and it weakens the hepatic ability to remove LDL-C from the blood. 2019 European Society of Cardiology/European Atherosclerosis Society (ESC/EAS) guidelines for the management of dyslipidemias reemphasize that if the combination of maximum statin and ezetimibe can't make the LDL-C reach the standard, then PCSK9 inhibitor is recommended to be added in the early stage for acute coronary syndrome (ACS) patients [8]. Its recommendation also highlights the maximum dose of statin and the early application of PCSK9

Abbreviations: PCSK9, proprotein convertase subtilisin/kexin type 9; CVD, cardiovascular disease; LDL-C, low-density lipoprotein cholesterol; LDLRs, low-density lipoprotein receptors; ESC/EAS, European Society of Cardiology/European Atherosclerosis Society; ACS, acute coronary syndrome; GPs, *G. pentaphyllum* saponin; DMEM, Dulbecco's modified Eagle's medium; FBS, fetal bovine serum; MTT, 3-[4, 5-Dimethythylthiazol-2-yl]-2, 5-diphenyltetrazolium bromide; LPDS, lipoprotein deficient serum.

* Corresponding authors.
E-mail addresses: zhangjian@jsatcm.com (J. Zhang), cpu-yzq@cpu.edu.cn (Z.-Q. Yin), kpan@cpu.edu.cn (K. Pan).
[1] These authors contributed equally to this work.

https://doi.org/10.1016/j.bioorg.2021.104843
Received 3 February 2021; Received in revised form 16 March 2021; Accepted 16 March 2021
Available online 1 April 2021

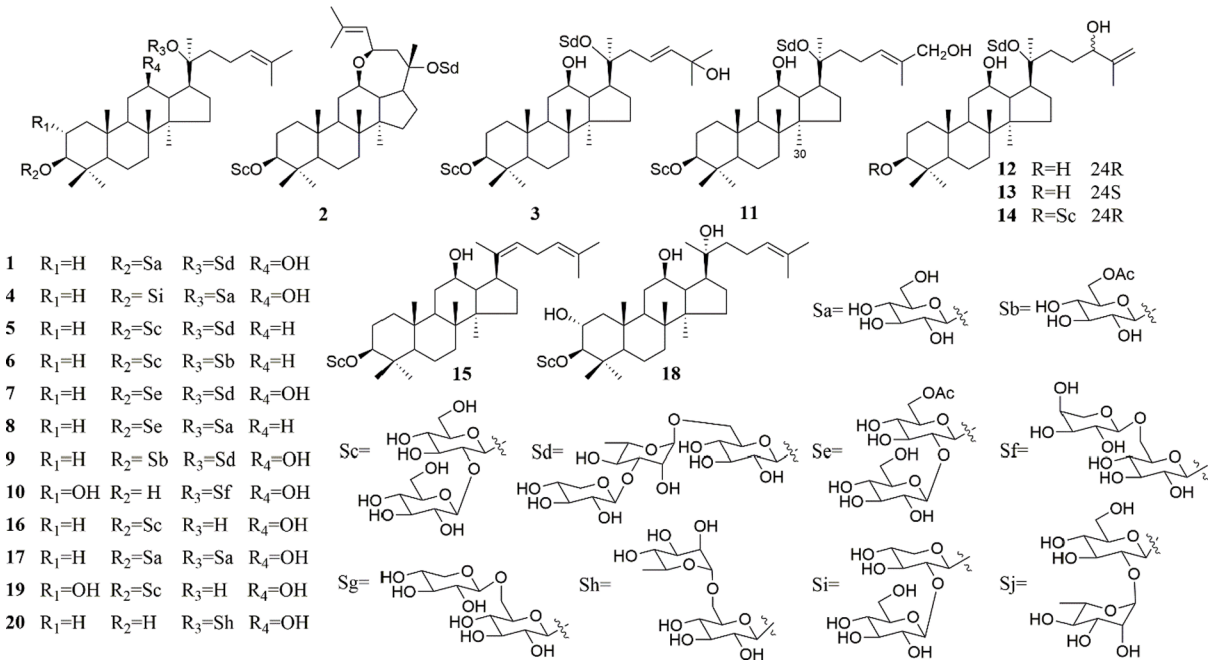

Fig. 1. Structures of compounds **1**–**20**.

inhibitors. Thus, PCSK9 inhibitors offer a novel therapeutic model against LDL-C and are seen as the biggest advance in lipid-lowering since statins are discovered [9].

Previous researches have reported that *G. pentaphyllum* saponin (GPs) play a lipid-lowering role in inhibiting the expression of PCSK9 while increasing the expression of LDLRs in liver. Besides, the utilization of GPs combined with the statin therapy can further reduce LDL-C levels [10]. However, the specific active compounds from GPs toward PCSK9 inhibitors are still unclear. In order to discover lipid-lowering compounds from *G. pentaphyllum*, fourteen new triterpenoid saponins (**1**–**14**) and six known compounds (**15**–**20**) were purified (Fig. 1). Herein we reported the isolation and structural elucidation of saponins **1**–**20**, as well as their individual inhibitory effects of PCSK9.

2. Materials and methods

2.1. Apparatus and conditions

Optical rotations were measured at 589 nm in CH_3OH on a Rudolph Autopol IV polarimeter with a sodium lamp (Rudolph Research Analytical, USA). Infrared (IR) spectra were recorded on a Bruker Tensor 27 spectrometer (Bruker, Germany). NMR spectra were obtained from a Bruker Avance-300 and Bruker Avance-500 (Bruker, Germany) with TMS as internal standard. HRESIMS were performed on a Waters Q-TOF Micro^{TM} mass spectrometer (Waters, Milford, MA, USA). Agilent 1260 Infinity equipped with UV (Agilent, USA) and Alltech 3300 ELSD detector was used to analyze the samples, and SSI/LabAlliance semi preparative HPLC (Scientific Systems Inc., USA) was applied for further purification.

2.2. Materials and reagents

The total saponin extract of *G. pentaphyllum* (No. T20170303) from Guangxi resource is provided by Hunan Huabaotong Pharmaceutical Co., Ltd, Changsha, which is applied to product the granules of GPs for the treatment of hyperlipidemia. The original plant is identified as the whole plant of *Gynostemma pentaphyllum* (Thunb.) Makino by Professor Minjian Qin of China Pharmaceutical University. A voucher specimen (20161108) was deposited in Hunan Huabaotong Pharmaceutical Co., Ltd. A pack COSMOSIL 5C_{18}-AR-II column (250 mm × 20 mm, 5 μm), Silica gel (Qingdao Marine Chemical Factory of China, Qingdao, China), and C_{18} reverse phase silica gel (YMC, Tokyo, Japan) were used for column chromatography. Thin-layer chromatography (TLC) was displayed with Merck silica gel 60 F254 and Merck ODS RP-18 gel (Merck, Darmstadt, Germany). Dulbecco's modified Eagle's medium (DMEM, low glucose), fetal bovine serum (FBS), and 1 × PBS (pH 7.4) were purchased from Gibco (Life Technologies, Carlsbad, CA). MTT assay was obtained from KeyGEN BioTECH (Jiangsu, China). PCSK9 ELISA kits were obtained from Jiangsu Meibiao BioTECH (Yancheng, China). All solvents used for isolation were of analytical grade, for HPLC analysis were of chromatographic grade.

2.3. Extraction and isolation

The whole herb of *G. pentaphyllum* (10 kg) were triturated and then extracted with water (2 × 80 L, 2 h for each time) by decocting method. After filtration and concentration, the water extract was subjected to a D-101 macroporous resin column eluted with ethanol. Then the above fraction was mainly enriched in the saponins, which was decolorized through alumina column to obtain the total saponin extract (254 g) after concentration, vacuum drying and crushing. The total saponin extract (70 g) of *G. pentaphyllum* were extracted with methanol three times (560 mL, 0.5 h for each time) by ultrasonic. Methanol insoluble and soluble parts were obtained by filtration and concentration. The methanol soluble fraction (60 g) was subjected to a silica gel eluting with $CHCl_3$-MeOH-H_2O gradient (100:0:0→0:100:0) to obtain nine fractions (Fr.2a ~ Fr.2i). Fr.2c was further separated by C_{18} reverse phase silica gel column eluting with MeOH-H_2O gradient (20:80→100:0) to three fractions (Fr.2c1 ~ Fr.2c3). Then, Fr.2c1 ~ Fr.2c3 were separated over pre-HPLC (ACN/H_2O = 31/69, 45/55, 53/47; flow rate: 10 mL/min) to get compounds **7** (5.5 mg; t_R = 21 min); **16** (51.7 mg; t_R = 45 min), **17** (6.0 mg; t_R = 20 min); **15** (18.4 mg; t_R = 57 min), **20** (19.1 mg; t_R = 42 min), respectively. Fr.2d was subjected to C_{18} reverse phase silica gel column eluting with MeOH-H_2O gradient (15:85→100:0) to five fractions (Fr.2d1 ~ Fr.2d5). Then, Fr.2d2 ~ Fr.2d3 and Fr.2d5 were separated over pre-HPLC (ACN/H_2O = 34/66, 35/65, 35/65; flow rate: 10 mL/min) to get compounds **13** (5.5 mg; t_R = 41 min); **4** (17.0 mg; t_R = 26 min), **12** (6.5 mg; t_R = 30 min); **10** (6.2 mg; t_R = 20 min), respectively.

Table 1
1H and 13C NMR Data for Compounds **1**–**5**.

No.	1		2		3		4		5	
	δ_H [a]	δ_C [b]	δ_H [a]	δ_C [b]	δ_H [a]	δ_C [b]	δ_H [a]	δ_C [b]	δ_H [a]	δ_C [b]
1	1.61, 0.82	39.6	1.54, 0.88	39.8	1.60, 0.74 (m)	39.5	1.69, 0.87	39.6	1.52, 0.82 (m)	39.7
2	1.81, 1.36	27.1	2.22, 1.83	27.1	2.19 (m), 1.81	27.1	2.12(m), 1.85	27.0	2.25 (m), 1.84	26.1
3	3.37 (dd, 4.5,12.0)	89.2	3.34 (dd, 4.0,11.5)	89.2	3.27 (dd, 4.5,11.5)	89.4	3.25 (dd, 4.5,12.0)	89.1	3.34 (dd, 4.5,11.5)	89.4
4	—	40.1	—	40.1	—	40.0	—	40.1	—	40.1
5	0.75 (m)	56.8	0.72 (d, 11.5)	56.8	0.67 (m)	56.8	0.74 (m)	56.8	0.71 (m)	56.8
6	1.51, 1.38	18.8	1.48, 1.38	18.8	1.50, 1.37	18.8	1.52, 1.38	18.8	1.51, 1.38	18.8
7	1.51, 1.23 (m)	35.5	1.42, 1.22	35.6	1.50, 1.20 (m)	35.4	1.50, 1.22	35.5	1.51, 1.23 (m)	36.1
8	—	40.5	—	40.2	—	40.4	—	40.4	—	40.8
9	1.40	50.6	1.51	51.0	1.36	50.5	1.45	50.6	1.35	51.1
10	—	37.4	—	37.4	—	37.3	—	37.4	—	37.4
11	2.23, 1.87	31.1	1.94 (d, 12.5), 1.34	30.5	1.99, 1.55	31.2	2.03, 1.55	31.3	1.46, 1.22	22.3
12	4.20	70.5	3.67 (m)	80.1	4.04	70.8	4.14	70.6	2.02, 1.94	26.2
13	1.99 (t, 10.5)	49.9	1.58	50.2	2.03	49.9	2.00	49.9	1.89	43.1
14	—	51.8	—	51.7	—	51.8	—	51.8	—	51.4
15	1.52, 0.99	31.2	1.54, 1.13	32.9	1.59, 0.95	30.9	1.59, 1.01	31.2	1.60, 1.10	31.9
16	1.99, 1.36	27.1	2.24, 2.13 (m)	25.9	1.78, 1.44	26.8	1.88, 1.38	27.2	2.06,1.44	27.2
17	2.61 (m)	51.8	3.13 (td, 4.5, 10.5)	47.1	2.50	51.9	2.57	52.1	2.24	49.3
18	0.96 (s)	16.4	0.96 (s)	15.9	1.03 (s)	16.4	0.97 (s)	16.4	1.01 (s)	16.1
19	0.82 (s)	16.7	0.82 (s)	16.8	0.83 (s)	16.6	0.86 (s)	16.7	0.82 (s)	16.9
20	—	83.8	—	82.4	—	83.7	—	83.7	—	82.8
21	1.67 (s)	22.4	1.50 (s)	24.8	1.62 (s)	23.4	1.62 (s)	22.7	1.52 (s)	21.4
22	2.39, 1.79	36.5	2.81 (d, 16.0), 2.25	52.7	3.09 (dd, 5.5,14.0), 2.77 (m)	40.1	2.39(m), 1.84	36.5	2.05, 1.95	41.1
23	2.64, 2.39	23.3	4.82 (t, 8.0)	72.7	6.22 (m)	123.1	2.50, 2.25 (m)	23.6	2.53, 2.46	23.5
24	5.32 (m)	126.4	5.53 (d, 7.0)	129.6	6.07 (d, 15.5)	142.7	5.25 (m)	126.3	5.43 (m)	126.6
25	—	131.4	—	131.7	—	70.3	—	131.3	—	131.0
26	1.61 (s)	26.2	1.65 (s)	26.0	1.57 (s)	30.9	1.62 (s)	26.1	1.72 (s)	26.2
27	1.68 (s)	18.3	1.83 (s)	19.2	1.57 (s)	30.9	1.62 (s)	18.1	1.73 (s)	18.3
28	1.30 (s)	28.5	1.30 (s)	28.4	1.28 (s)	28.4	1.28 (s)	28.5	1.30 (s)	28.4
29	1.00 (s)	17.2	1.10 (s)	16.9	1.09 (s)	16.9	1.11 (s)	16.9	1.12 (s)	17.3
30	1.00 (s)	17.9	1.09 (s)	17.3	0.92 (s)	17.6	0.95 (s)	17.7	1.01 (s)	17.0
	3-Glc		3-Glc		3-Glc		3-xyl		3-Glc	
1′	4.93 (d, 8.0)	107.3	4.93 (d, 7.5)	105.4	4.90 (d, 7.5)	105.4	4.83 (d, 6.5)	106.1	4.94 (d, 7.5)	105.4
2′	4.02	76.2	4.21	83.8	4.23	83.7	4.20	83.6	4.24	83.8
3′	4.23	79.1	4.28	78.7	4.29	78.6	4.22	78.4	4.32	78.8
4′	4.18	72.3	4.11	72.0	4.14	71.4	4.15	71.3	4.14	72.4
5′	3.99	78.8	3.92	78.6	3.90	78.4	4.29, 3.67 (m)	67.0	3.92	78.7
6′	4.59, 4.38	63.5	4.54, 4.31	63.1	4.55, 4.31	63.2			4.57, 4.35	63.1
			Glc		Glc		Glc		Glc	
1′’			5.35 (d, 7.5)	106.4	5.36 (d, 8.0)	106.3	5.35 (d, 7.5)	106.4	5.36 (d, 7.5)	106.4
2′’			4.11	77.4	4.11	77.4	4.11	77.4	4.10	77.0
3′’			4.28	78.3	4.23	78.3	4.25	78.4	4.24	78.4
4′’			4.32	72.1	4.31	72.1	4.33	72.0	4.31	72.4
5′’			3.92	78.3	3.91	78.6	3.93	78.6	3.94	78.6
6′’			4.51, 4.46	63.2	4.48, 4.43	63.1	4.49, 4.46	63.1	4.48, 4.46	63.3
	20-Glc		20-Glc		20-Glc		20-Glc		20-Glc	
1′’’	5.11 (d, 7.5)	98.5	5.10 (d, 7.5)	99.7	5.14 (d, 7.5)	98.6	5.18 (d, 7.5)	98.6	5.03 (d, 7.5)	99.2
2′’’	3.96	75.4	3.94	75.7	3.94	75.5	3.98 (m)	75.5	3.98	76.0
3′’’	4.18	79.9	4.20	79.2	4.15	79.4	4.22	79.6	4.21	79.4
4′’’	3.90	72.3	3.96	72.3	3.90	72.1	4.15	72.1	3.95	72.1
5′’’	3.98	77.2	4.05	77.2	4.00	77.3	3.92	78.6	4.00	77.5
6′’’	4.63 (m), 4.02	68.3	4.69, 4.05	68.9	4.58, 4.04	67.9	4.33, 4.31	63.3	4.66 (m), 4.04	69.0
	Rha		Rha		Rha				Rha	
1′’’’	5.42 (br s)	102.4	5.45 (br s)	102.9	5.46 (br s)	102.3			5.44 (br s)	102.9
2′’’’	4.73 (m)	72.2	4.79 (m)	71.9	4.71 (m)	72.0			4.77 (m)	72.1
3′’’’	4.54	83.7	4.51	83.8	4.53	83.3			4.54	83.9
4′’’’	4.38	73.4	4.40 (t, 9.0)	73.3	4.33	73.4			4.41 (m)	73.4
5′’’’	4.32 (m)	70.0	4.33	69.9	4.31	69.8			4.34	69.9
6′’’’	1.57 (d, 6.5)	18.9	1.60 (d, 6.5)	18.9	1.56 (d, 6.5)	18.8			1.60 (d, 6.0)	18.9
	Xyl		Xyl		Xyl				Xyl	
1′’’’’	5.24 (d, 7.5)	107.8	5.18 (d, 8.0)	107.6	5.23 (d, 8.0)	107.5			5.19 (d, 8.0)	107.7
2′’’’’	4.02	76.0	4.00	76.1	4.00	75.9			4.01	76.1
3′’’’’	4.12	78.7	4.09	78.7	4.11	78.7			4.13	78.3
4′’’’’	4.17	71.5	4.15	71.4	4.14	71.4			4.15	71.4
5′’’’’	4.32, 3.66 (m)	67.8	4.32, 3.62	67.8	4.28, 3.63 (t, 10.0)	67.6			4.30, 3.63 (m)	67.7

[a] Measured at 500 MHz; signals overlapping are not labeled; *J* values in parentheses
[b] Measured at 125 MHz

The Fr.2d4 was subjected to C_{18} reverse phase silica gel column eluting with MeOH-H_2O gradient (35:65→100:0) to two fractions (Fr.2d4a ~ Fr.2d4b). Then, Fr.2d4a ~ Fr.2d4b were separated by pre-HPLC (ACN/H_2O = 37/63, 40/60; flow rate: 10 mL/min) to get compounds **6** (5.5 mg; t_R = 31 min); **9** (6.5 mg; t_R = 15 min), **18** (6.2 mg; t_R = 23 min), **19** (5.5 mg; t_R = 33 min), respectively. Fr.2h was further separated by C_{18} reverse phase silica gel column eluting with MeOH-H_2O gradient (5:95→100:0) to five fractions (Fr.2h1 ~ Fr.2h5). Then, Fr.2h3 ~ Fr.2h5 were separated by pre-HPLC (ACN/H_2O = 21/79, 31/69, 33/67; flow rate: 10 mL/min) to get compounds **2** (42.1 mg; t_R = 36 min); **1** (35.1

Table 2
^{1}H and ^{13}C NMR Data for Compounds **6**–**10**.

No.	6		7		8		9		10	
	δ_H [a]	δ_C [b]	δ_H [a]	δ_C [b]	δ_H [a]	δ_C [b]	δ_H [a]	δ_C [b]	δ_H [a]	δ_C [b]
1	1.51, 0.80	39.7	1.73, 0.91 (m)	39.6	1.66, 0.97	39.8	1.74, 0.93	39.6	2.38, 1.23 (m)	48.8
2	2.23, 1.87	27.1	2.20 (m), 1.88	27.1	2.25 (m), 1.95	27.2	2.25 (m), 1.91	27.1	4.09	69.2
3	3.30 (dd, 4.5,12.0)	89.4	3.25 (dd, 4.0,11.5)	89.8	3.29 (dd, 4.5,12.0)	89.8	3.34 (dd, 4.0,11.5)	89.7	3.36 (d, 9.0)	84.1
4	—	40.1	—	40.1	—	40.2	—	40.0	—	40.3
5	0.71 (m)	56.8	0.72 (m)	56.9	0.76 (m)	56.9	0.78 (m)	56.9	0.97	56.9
6	1.50, 1.39	18.8	1.50, 1.38	18.8	1.50, 1.40	18.9	1.51, 1.37	18.9	1.56, 1.47	19.2
7	1.50, 1.24 (m)	36.0	1.48, 1.21 (m)	35.5	1.50, 1.25	36.1	1.52, 1.23 (m)	35.5	1.50, 1.25	35.5
8	—	40.5	—	40.4	—	41.1	—	40.5	—	40.5
9	1.31	51.0	1.44	50.6	1.38	51.5	1.46	50.7	1.57	50.8
10	—	37.3	—	37.4	—	37.5	—	37.4	—	38.9
11	1.44, 1.18	21.8	2.05, 1.53	31.2	1.58, 1.09	22.3	2.05, 1.50	31.3	2.14, 1.58	31.4
12	2.05, 1.94	25.9	4.21	70.5	2.08, 1.96	25.9	4.20	70.5	4.17	70.5
13	1.93	42.9	1.99	49.9	1.96	43.0	1.97 (m)	49.9	1.99 (t, 10.5)	49.9
14	—	51.3	—	51.8	—	51.1	—	51.9	—	51.8
15	1.59, 1.08	31.9	1.57, 0.99	31.1	1.60, 1.09	31.9	1.61, 0.98	31.1	1.59, 1.00	31.1
16	2.04, 1.40	28.4	1.86, 1.36	27.1	2.04, 1.25	28.5	1.87, 1.32	27.1	1.84, 1.33	27.0
17	2.20 (m)	49.0	2.61 (m)	51.8	2.20 (m)	48.9	2.62	51.8	2.56	52.1
18	0.98 (s)	16.0	0.97 (s)	16.4	1.01 (s)	16.2	0.97 (s)	16.6	0.98 (s)	16.5
19	0.80 (s)	16.8	0.85 (s)	16.6	0.84 (s)	16.9	0.85 (s)	16.4	0.97 (s)	18.0
20	—	82.7	—	83.8	—	82.7	—	83.8	—	83.9
21	1.48 (s)	22.3	1.67 (s)	22.3	1.52 (s)	22.0	1.68 (s)	22.3	1.63 (s)	22.6
22	2.00, 1.90	41.0	2.39, 1.78	36.5	2.02, 1.90	40.7	2.39, 1.77	36.5	2.39, 1.83	36.6
23	2.43, 2.43	23.5	2.64, 2.38	23.3	2.42, 2.42	23.6	2.65, 2.39	23.3	2.58, 2.37	23.6
24	5.35 (m)	126.4	5.32 (m)	126.4	5.31 (t, 7.0)	126.5	5.32 (m)	126.4	5.33 (m)	126.4
25	—	131.0	—	131.4	—	131.1	—	131.4	—	131.5
26	1.71 (s)	26.1	1.60 (s)	26.1	1.69 (s)	26.2	1.60 (s)	26.2	1.63 (s)	26.2
27	1.71 (s)	18.2	1.68 (s)	18.2	1.69 (s)	18.3	1.68 (s)	18.3	1.67 (s)	18.3
28	1.28 (s)	28.4	1.28 (s)	28.5	1.29 (s)	28.4	1.30 (s)	28.5	1.25 (s)	29.6
29	1.11 (s)	16.9	1.09 (s)	17.0	1.12 (s)	17.0	0.97 (s)	17.1	1.07 (s)	17.8
30	0.97 (s)	17.2	0.98 (s)	17.8	0.99 (s)	17.2	1.00 (s)	17.8	0.93 (s)	17.8
	3-Glc		3-Glc		3-Glc		3-Glc			
1′	4.92 (d, 8.0)	105.4	4.85 (d, 7.5)	105.4	4.87 (d, 7.5)	105.4	4.87 (d, 8.0)	107.3		
2′	4.22	83.6	4.20	83.5	4.22	83.6	4.01	76.0		
3′	4.29	78.7	4.25	78.4	4.31	78.4	4.20	78.9		
4′	4.14	72.0	3.96	71.8	4.23	72.5	4.03	72.1		
5′	3.92	78.4	3.95	75.0	3.98	75.0	4.04	75.4		
6′	4.55, 4.34	63.2	4.93, 4.73	64.7	4.94, 4.78 (m)	64.9	4.96 (m), 4.80 (dd, 5.5,11.5)	65.1		
$\underline{C}H_3CO$			2.03 (s)	21.2	2.06 (s)	21.2	2.02 (s)	21.2		
$CH_3\underline{C}O$			—	171.2	—	171.2	—	171.2		
	Glc		Glc		Glc					
1′’	5.36 (d, 7.5)	106.2	5.36 (d, 8.0)	106.4	5.37 (d, 7.5)	106.4				
2′’	4.11	77.3	4.11	77.4	4.12 (m)	77.4				
3′’	4.22	78.3	4.24	78.5	4.26	78.7				
4′’	4.30	72.1	4.29	72.1	4.32	72.1				
5′’	3.91	78.5	3.93	78.7	3.93	78.5				
6′’	4.47, 4.43	63.1	4.48, 4.46	63.1	4.49, 4.48	63.2				
	20-Glc		20-Glc		20-Glc		20-Glc		20-Glc	
1′’’	5.01 (br s)	98.8	5.10 (d, 7.5)	98.4	5.09 (br s)	99.0	5.11 (d, 7.5)	98.4	5.10 (d, 7.5)	98.5
2′’’	3.96	75.1	3.95	75.3	4.00	76.1	3.96	75.3	3.93 (t, 8.0)	75.3
3′’’	4.17	79.1	4.18	79.9	4.23	79.4	4.18	80.0	4.16	79.7
4′’’	3.95	72.1	3.90	72.3	3.98	71.8	3.90 (m)	72.4	4.04	72.3
5′’’	3.96	75.8	3.98	77.1	3.96	78.2	3.99	77.2	4.02	77.1
6′’’	4.95, 4.62 (m)	65.5	4.63 (d, 9.0), 4.01	68.3	4.38, 4.27	63.6	4.63 (d, 9.0), 4.00	68.3	4.69 (m), 4.24	69.7
$\underline{C}H_3CO$	2.08 (s)	21.2								
$CH_3\underline{C}O$	—	171.2								
			Rha				Rha		Ara	
1′’’’			5.42 (br s)	102.5			5.42 (br s)	102.5	4.98 (d, 6.0)	105.1
2′’’’			4.73 (m)	72.2			4.74 (m)	72.2	4.44 (m)	72.6
3′’’’			4.53	83.7			4.54 (m)	83.7	4.21	74.5
4′’’’			4.39 (t, 9.5)	73.4			4.40 (t, 9.5)	73.4	4.36 (m)	69.0
5′’’’			4.32	70.0			4.32	70.0	4.30, 3.78 (dd, 2.0,12.0)	66.0
6′’’’			1.57 (d, 6.0)	18.9			1.57 (d, 6.0)	18.9		
			Xyl				Xyl			
1′’’’’			5.24 (d, 7.5)	107.8			5.24 (d, 7.5)	107.8		
2′’’’’			4.03	76.0			4.05	76.0		
3′’’’’			4.13	78.7			4.14 (m)	78.7		
4′’’’’			4.18	71.4			4.17	71.5		
5′’’’’			4.32, 3.66 (t, 10.5)	67.7			4.33, 3.66 (t, 11.0)	67.7		

[a] Measured at 500 MHz; signals overlapping are not labeled; *J* values in parentheses;

[b] Measured at 125 MHz

Table 3
^{1}H and ^{13}C NMR Data for Compounds **11**–**14**.

No.	11		12		13		14	
	δ_H [a]	δ_C [b]	δ_H [a]	δ_C [b]	δ_H [a]	δ_C [b]	δ_H [a]	δ_C [b]
1	1.57, 0.74 (m)	39.5	1.70 (m), 0.91	39.8	1.71 (m), 0.91	39.8	1.55, 0.74 (m)	39.6
2	2.20 (m), 1.83	27.1	1.86, 1.82	28.6	1.86, 1.82	28.6	2.19 (m), 1.84	27.1
3	3.27 (dd, 4.0,11.5)	89.4	3.42 (dd, 5.0,10.5)	78.5	3.41 (dd, 5.5,11.0)	78.5	3.27 (dd, 4.5,11.5)	89.4
4	—	40.0	—	39.9	—	39.9	—	40.0
5	0.66 (m)	56.7	0.81 (m)	56.8	0.80 (m)	56.8	0.67 (m)	56.8
6	1.50, 1.35	18.7	1.56, 1.46	19.2	1.56, 1.45	19.2	1.49, 1.36	18.8
7	1.47, 1.20 (m)	35.4	1.54, 1.25	35.6	1.53, 1.24	35.6	1.49, 1.19	35.5
8	—	40.3	—	40.4	—	40.5	—	40.4
9	1.35	50.5	1.46	50.7	1.45	50.7	1.37	50.6
10	—	37.2	—	37.7	—	37.8	—	37.3
11	1.96, 1.48	31.1	2.04, 1.55	31.4	2.04, 1.54	31.3	1.95, 1.53	30.6
12	4.18	70.5	4.15	70.7	4.18	70.7	4.16	70.7
13	1.96	49.8	2.06	49.9	2.08	49.8	2.05	49.8
14	—	51.8	—	50.8	—	51.8	—	51.8
15	1.53, 0.96	31.0	1.55, 0.98	31.1	1.54, 0.97	31.1	1.53, 0.97	31.0
16	1.83, 1.35	27.0	1.87, 1.40(m)	27.1	1.87, 1.38(m)	27.1	1.94, 1.38	27.1
17	2.59 (m)	51.8	2.58	52.0	2.59	52.1	2.58 (m)	52.0
18	0.94 (s)	16.3	1.03 (s)	16.4	0.98 (s)	16.5	0.98 (s)	16.3
19	0.81 (s)	16.6	0.89 (s)	16.7	0.88 (s)	16.7	0.81 (s)	16.6
20	—	83.6	—	83.9	—	84.1	—	83.9
21	1.67 (s)	22.4	1.69 (s)	22.7	1.67 (s)	22.7	1.68 (s)	22.7
22	2.42, 1.82	36.3	2.59, 1.94	33.0	2.46, 2.18	33.0	2.57 (m), 1.92	33.0
23	2.71, 2.46	22.9	2.33, 2.08	30.7	2.34, 2.06	30.8	2.31 (m), 2.04	31.3
24	5.80 (t, 6.5)	125.9	4.47 (t, 6,0)	76.4	4.46 (dd, 4.5,7.5)	76.4	4.47	76.3
25	—	136.6	—	149.9	—	150.2	—	149.8
26	4.22, 4.22	68.4	5.26 (s), 4.93	110.7	5.23(s), 4.89	110.6	5.25 (s), 4.92 (m)	110.7
27	1.88 (s)	14.4	1.96 (s)	18.5	1.96(s)	18.7	1.95 (s)	18.5
28	1.27 (s)	28.4	1.22 (s)	29.0	1.22 (s)	29.1	1.28 (s)	28.5
29	1.09 (s)	16.9	1.03 (s)	16.7	1.03 (s)	16.7	1.09 (s)	16.9
30	0.97 (s)	17.7	0.95 (s)	17.8	0.95 (s)	17.8	0.96 (s)	17.7
	3-Glc						3-Glc	
1′	4.90 (d, 7.5)	105.4					4.90 (d, 7.5)	105.4
2′	4.20	83.8					4.22	83.8
3′	4.30	78.7					4.31	78.7
4′	4.13	72.0					4.12	72.0
5′	3.90	78.4					3.91	78.6
6′	4.54, 4.31	63.2					4.55, 4.30	63.1
	Glc						Glc	
1′’	5.35 (d, 7.5)	106.2					5.35 (d, 7.5)	106.4
2′’	4.10	77.3					4.11	77.4
3′’	4.23	78.6					4.25	78.4
4′’	4.30	72.0					4.31	72.1
5′’	3.90	78.3					3.93	78.3
6′’	4.47, 4.44	63.1					4.54, 4.46	63.2
	20-Glc		20-Glc		20-Glc		20-Glc	
1′’’	5.10 (d, 7.5)	98.3	5.10 (d, 7.5)	98.5	5.11 (d, 8.0)	98.5	5.10 (d, 8.0)	98.4
2′’’	3.96	75.3	3.92	75.4	3.94	75.4	3.92	75.3
3′’’	4.17	79.8	4.16	79.7	4.18	79.8	4.17	79.7
4′’’	3.88	72.3	3.87	72.3	3.88	72.4	3.86	72.3
5′’’	3.98	77.1	3.96	77.1	3.98	77.2	3.97	77.1
6′’’	4.62 (m), 4.00	68.3	4.62 (m), 4.00	68.4	4.63 (m), 4.02	68.3	4.62 (m), 3.99	68.4
	Rha		Rha		Rha		Rha	
1′’’’	5.41 (br s)	102.4	5.44 (br s)	102.6	5.45 (br s)	102.6	5.44 (br s)	102.6
2′’’’	4.73 (m)	72.1	4.78 (m)	72.1	4.77 (m)	72.1	4.77 (m)	72.1
3′’’’	4.53	83.4	4.55 (dd, 3.0,9.0)	83.5	4.55 (dd, 3.0,9.5)	83.6	4.54	83.4
4′’’’	4.37 (t, 9.5)	73.2	4.39 (t, 9.0)	73.4	4.40 (t, 9.0)	73.4	4.39 (t, 9.0)	73.4
5′’’’	4.30	69.9	4.32	69.9	4.31	70.0	4.32	69.9
6′’’’	1.56 (d, 6.0)	18.8	1.59 (d, 6.0)	18.9	1.58 (d, 6.0)	18.9	1.57 (d, 6.0)	18.9
	Xyl		Xyl		Xyl		Xyl	
1′’’’’	5.24 (d, 7.5)	107.6	5.25 (d, 8.0)	107.7	5.26 (d, 7.5)	107.8	5.24 (d, 7.5)	107.6
2′’’’’	4.02	75.9	4.03	76.0	4.03	76.0	4.02	75.9
3′’’’’	4.12	78.5	4.12 (t, 8.5)	78.7	4.13 (t, 8.5)	78.7	4.12	78.6
4′’’’’	4.18	71.4	4.19	71.4	4.16	71.5	4.17	71.4
5′’’’’	4.31, 3.66 (t, 11.0)	67.6	4.32, 3.66 (t, 11.0)	67.7	4.34, 3.67 (t, 11.0)	67.7	4.32, 3.65 (t, 10.0)	67.7

[a] Measured at 500 MHz; signals overlapping are not labeled; *J* values in parentheses.
[b] Measured at 125 MHz.

mg; t_R = 38 min), **5** (35.7 mg; t_R = 27 min); **8** (5.8 mg; t_R = 40 min), respectively. Fr.2i was further separated by C_{18} reverse phase silica gel column eluting with MeOH-H_2O gradient (15:85 →100:0) to three fractions (Fr.2i1 ~ Fr.2i3). Then, Fr.2i1 was separated on a silica gel column chromatography with $CHCl_3$-MeOH-H_2O (100:40:4), and the subfraction was further separated by pre-HPLC (ACN/H_2O = 25/75; flow rate: 10 mL/min) to obtain compounds **3** (24.5 mg; t_R = 28 min), **11** (8.1 mg; t_R = 30 min), **14** (7.2 mg; t_R = 35 min). The entire process of extraction and purification was shown in Supporting Information.

2.3.1. Gypenoside LXXXVIII (1)

White amorphous powder (MeOH); $[\alpha]_D^{20}$ + 1.57 (*c* 0.51, MeOH); IR (KBr): ν_{max} 3395, 2918, 1599, 1077 cm^{-1}; HRESIMS: *m/z* 1085.5858 [M + Na]$^+$ (calcd for $C_{53}H_{90}O_{21}Na$, 1085.5872); NMR data, see Table 1.

2.3.2. Gypenoside LXXXIX (2)

White amorphous powder (MeOH); $[\alpha]_D^{20}$ −33.0 (*c* 0.11, MeOH); IR (KBr): ν_{max} 3397, 2920, 1659, 1079 cm^{-1}; HRESIMS: *m/z* 1221.6276 [M - H]$^-$ (calcd for $C_{59}H_{97}O_{26}$, 1221.6268); NMR data, see Table 1.

2.3.3. Gypenoside XC (3)

White amorphous powder (MeOH); $[\alpha]_D^{20}$ −10.6 (*c* 0.11, MeOH); IR (KBr): ν_{max} 3397, 2921, 1659, 1078 cm^{-1}; HRESIMS: *m/z* 1239.6373 [M - H]$^-$ (calcd for $C_{59}H_{99}O_{27}$, 1239.6374); NMR data, see Table 1.

2.3.4. Gypenoside XCI (4)

White amorphous powder (MeOH); $[\alpha]_D^{20}$ + 13.6 (*c* 0.12, MeOH); IR (KBr): ν_{max} 3397, 2920, 1659, 1078 cm^{-1}; HRESIMS: *m/z* 915.5326 [M - H]$^-$ (calcd for $C_{47}H_{79}O_{17}$, 915.5317); NMR data, see Table 1.

2.3.5. Gypenoside XCII (5)

White amorphous powder (MeOH); $[\alpha]_D^{20}$ −25.5 (*c* 0.11, MeOH); IR (KBr): ν_{max} 3363, 2937, 1650, 1597, 1041 cm^{-1}; HRESIMS: *m/z* 1231.6431 [M + Na]$^+$ (calcd for $C_{59}H_{100}O_{25}Na$, 1231.6446); NMR data, see Table 1.

2.3.6. Gypenoside XCIII (6)

White amorphous powder (MeOH); $[\alpha]_D^{20}$ + 11.4 (*c* 0.12, MeOH); IR (KBr): ν_{max} 3397, 2920, 1744, 1642, 1078 cm^{-1}; HRESIMS: *m/z* 971.5586 [M - H]$^-$ (calcd for $C_{50}H_{83}O_{18}$, 971.5579); NMR data, see Table 2.

2.3.7. Gypenoside XCIV (7)

White amorphous powder (MeOH); $[\alpha]_D^{20}$ −1.5 (*c* 0.12, MeOH); IR (KBr): ν_{max} 3398, 2925, 1742, 1642, 1079 cm^{-1}; HRESIMS: *m/z* 1265.6541 [M - H]$^-$ (calcd for $C_{61}H_{101}O_{27}$, 1265.6530); NMR data, see Table 2.

2.3.8. Gypenoside XCV (8)

White amorphous powder (MeOH); $[\alpha]_D^{20}$ −3.0 (*c* 0.11, MeOH); IR (KBr): ν_{max} 3302, 2927, 1743, 1653, 1076 cm^{-1}; HRESIMS: *m/z* 971.5572 [M - H]$^-$ (calcd for $C_{50}H_{83}O_{18}$, 971.5579); NMR data, see Table 2.

2.3.9. Gypenoside XCVI (9)

White amorphous powder (MeOH); $[\alpha]_D^{20}$ + 12.8 (*c* 0.12, MeOH); IR (KBr): ν_{max} 3397, 2943, 1729, 1642, 1598, 1077 cm^{-1}; HRESIMS: *m/z* 1103.5990 [M - H]$^-$ (calcd for $C_{55}H_{91}O_{22}$, 1103.6002); NMR data, see Table 2.

2.3.10. Gypenoside XCVII (10)

White amorphous powder (MeOH); $[\alpha]_D^{20}$ + 11.0 (*c* 0.11, MeOH); IR (KBr): ν_{max} 3329, 2922, 1601, 1049 cm^{-1}; HRESIMS: *m/z* 793.4714 [M + Na]$^+$ (calcd for $C_{41}H_{70}O_{13}Na$, 793.4714); NMR data, see Table 2.

2.3.11. Gypenoside XCVIII (11)

White amorphous powder (MeOH); $[\alpha]_D^{20}$ −24.7 (*c* 0.10, MeOH); IR (KBr): ν_{max} 3397, 2924, 1649, 1078 cm^{-1}; HRESIMS: *m/z* 1239.6368 [M - H]$^-$ (calcd for $C_{59}H_{99}O_{27}$, 1239.6374); NMR data, see Table 3.

2.3.12. Gypenoside XCIX (12)

White amorphous powder (MeOH); $[\alpha]_D^{20}$ −7.6 (*c* 0.11, MeOH); IR (KBr): ν_{max} 3397, 2942, 1649, 1077 cm^{-1}; HRESIMS: *m/z* 939.5311 [M + Na]$^+$ (calcd for $C_{47}H_{80}O_{17}Na$, 939.5293); NMR data, see Table 3.

2.3.13. Gypenoside C (13)

White amorphous powder (MeOH); $[\alpha]_D^{20}$ −13.0 (*c* 0.11, MeOH); IR (KBr): ν_{max} 3397, 2942, 1650, 1077 cm^{-1}; HRESIMS: *m/z* 939.5304 [M + Na]$^+$ (calcd for $C_{47}H_{80}O_{17}Na$, 939.5293); NMR data, see Table 3.

2.3.14. Gypenoside CI (14)

White amorphous powder (MeOH); $[\alpha]_D^{20}$ + 3.8 (*c* 0.12, MeOH); IR (KBr): ν_{max} 3398, 2941, 1649, 1078 cm^{-1}; HRESIMS: *m/z* 1239.6381 [M - H]$^-$ (calcd for $C_{59}H_{99}O_{27}$, 1239.6374); NMR data, see Table 3.

2.4. Acid hydrolysis of saponins 1–14 and HPLC analysis

Compounds **1**–**14** (3.0 mg each) dissolved in 2 M HCl (2.0 mL) and kept at 90℃ for 3 h, respectively. After cooling, each reaction mixture was diluted to 5 mL with water and then extracted with EtOAc (5 mL × 3). Each water layer was neutralized with 0.1 M NaOH. After concentration, the dried residue and standard monosaccharide (D-glucose, L-arabinose, D-xylose and L-rhamnose, 3.0 mg each) dissolved in pyridine (1 mL) containing of L-cysteine methyl ester hydrochloride (2 mg) and then kept at 60℃ for 1 h. Next, *o*-tolylisothiocyanate (2 mg) was added and the solution was kept at 60℃ for another 1 h. Finally, the reaction mixture was subjected to RP-HPLC for analysis. Agilent Extend-C_{18} column (250 × 4.6 mm, 5 μm); solvent, 25% CH_3CN for 30 min; flow rate, 1.0 mL/min; detector, UV; wavelength, 250 nm; column temperature, 30℃; injection volume, 10 μL. The derivatives of D-glucose, L-arabinose, D-xylose and L-rhamnose were detected at t_R (min) of 11.59, 13.37, 13.74 and 20.93 min, respectively.

2.5. Cell culture

Human hepatoma HepG2 cells were purchased from the Chinese Academy of Sciences (Shanghai, China). HepG2 cells were cultured in DMEM (low glucose), and media were supplemented with 10% FBS and 1% penicillin–streptomycin at 37℃ in a humid atmosphere with 5% CO_2.

2.6. Establishment of PCSK9 high expression model

The cell model was established by following the steps as below. The cells were inoculated in 12-well plates at 1 × 10^5 /well, which cultured in DMEM (low glucose) containing 10% FBS at 37℃ with 5% CO_2. After cell adherence, the media were replaced with DMEM containing 5% lipoprotein deficient serum (LPDS) and incubated for 23 h in the incubator. Next, 1 μM simvastatin was added to the cells and continue incubating for 1 h, and a PCSK9 high expression cell model was established.

2.7. Cell viability

The cytotoxicity of the isolates on HepG2 cells was performed by MTT. The cells were seeded and cultured in 96-well plates at 5 × 10^3 /well. when the cells approached confluence about 60%, the media were replaced with serum-free DMEM (low glucose) for 8 h fasting. After that, the cells were treated with different chemical compounds at 37℃ for 24 h and then the medium was removed. Twenty microliters of MTT (5 mg/mL) solution was added to each well. The MTT solution was removed

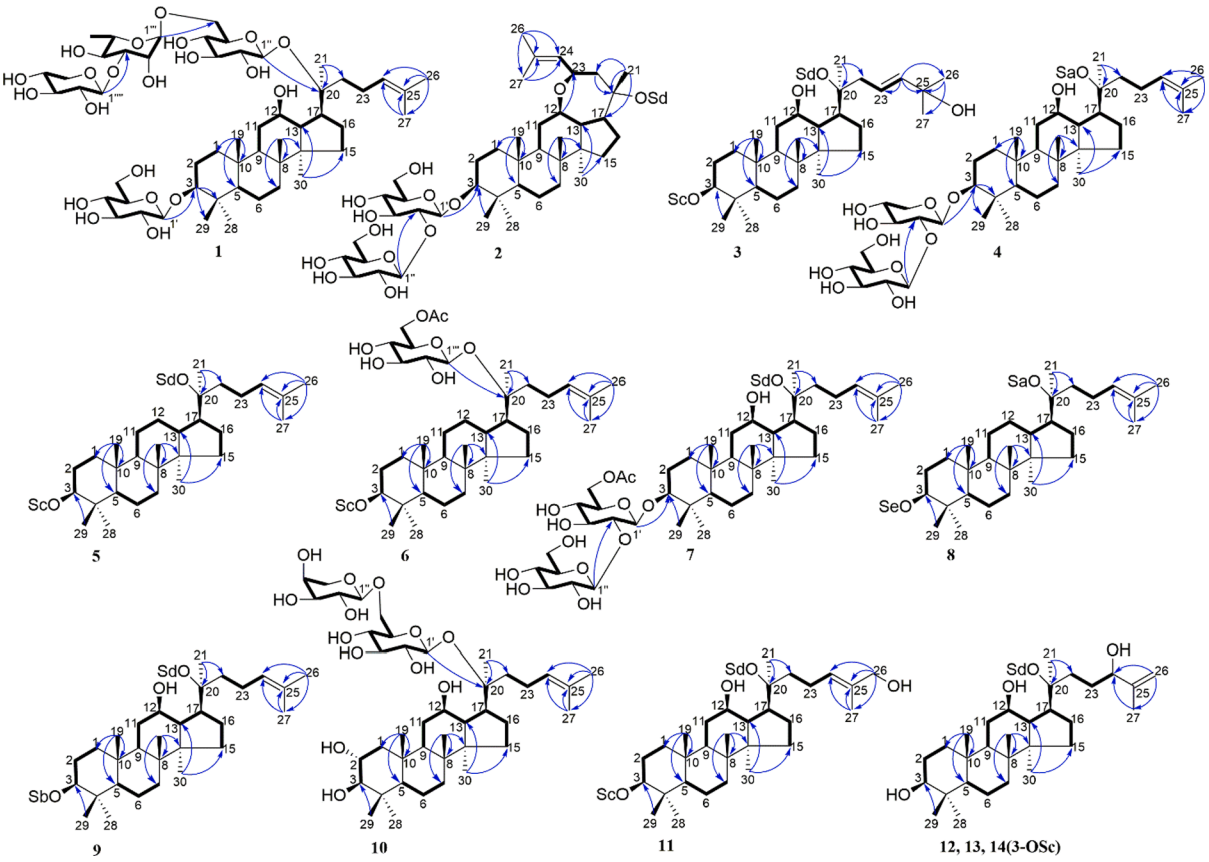

Fig. 2. Key ^{1}H–^{1}H COSY and selected HMBC correlations (H → C) of **1**–**14.**

after incubation for 4 h at 37C. The resultant formazan crystals in cells were solubilized with 150 μL of dimethyl sulfoxide and measured at 490 nm using a microplate reader. The dose of the compound is finalized according to the absorbance.

2.8. Inhibitory effect on PCSK9

HepG2 cells were divided into several groups with three parallel wells. The cells were inoculated in 12-well plates at 1×10^5 /well, which were cultured in DMEM (low glucose) containing 10% FBS at 37C with 5% CO_2. After cells adherence, these groups of cells were treated as follows: group one as the blank group, cultured with DMEM containing 5% FBS; group two (model group), group three (administration group), and group four (positive drug group) were all cultured with DMEM containing 5% lipoprotein deficient serum (LPDS). The blank group was treated for 48 h while the model and drug groups were cultured for 23 h

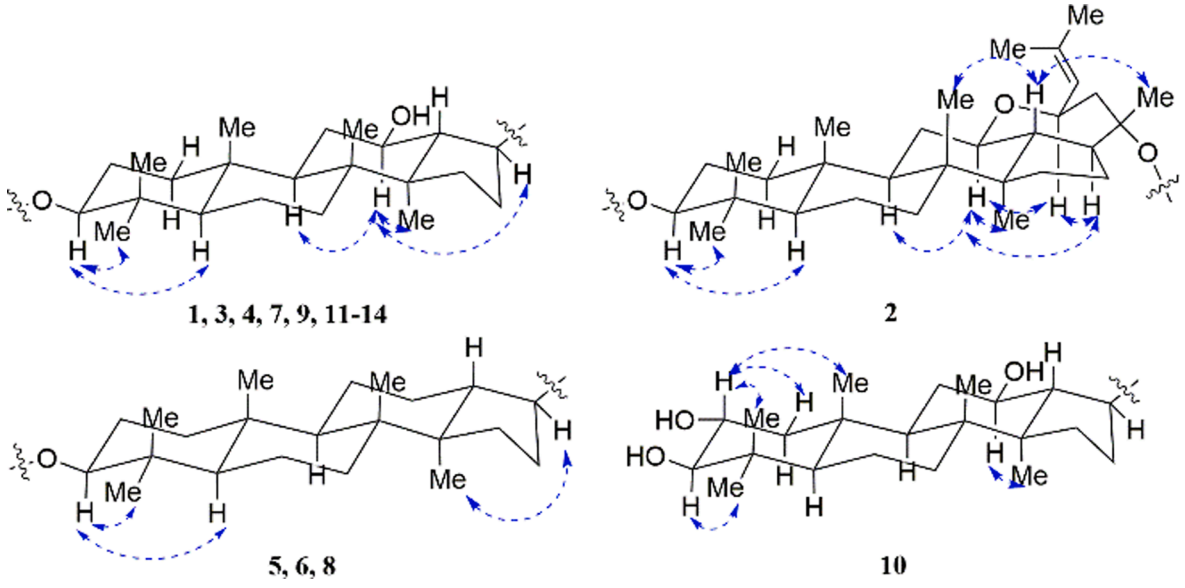

Fig. 3. Key NOESY correlations (H → H) of **1**–**14.**

before 1 h of simvastatin (1 μM) treatment. Then the model group was cultured for another 25 h. For drug groups, different compounds were added and then these groups were incubated for 24 h after 1 h of simvastatin treatment. After that, the supernatant was collected and the PCSK9 content in the cell supernatant was determined according to the ELISA kit instructions.

2.9. Statistical analysis

The experimental data were expressed as mean ± SD, and SPSS 22.0 was used for statistical analysis. The multigroup comparisons were analyzed by one-way analysis of variance (ANOVA), the homogeneity of variance was tested by LSD method or SNK method, and the heterogeneity was tested by non-parametric test (Kruskal-Wallis H test).

3. Results and discussion

Compound **1**, a white amorphous powder with a specific rotation of $[\alpha]_D^{20}$ + 1.57 (*c* 0.51, MeOH). Its molecular formula was determined as $C_{53}H_{90}O_{21}$ based on a HRESIMS ion at *m/z* 1085.5858 $[M + Na]^+$ (calcd 1085.5872). The IR spectrum suggested the presence of hydroxyl (3395 cm^{-1}) and olefinic bond (1599 cm^{-1}) functionalities. The ^{13}C NMR spectrum showed 53 carbon signals, of which 30 carbons were assigned to the aglycone and 23 carbons were assigned to four sugars. The presence of sugar units (D-glucose, L-rhamnose, D-xylose) in **1** was identified by the acid hydrolysis and HPLC analyses [11]. The ^1H NMR spectrum (Table 1) showed some characteristic signals for eight methyl groups, two oxygenated methines, one olefinic proton and four anomeric protons, and the coupling constant of the anomeric proton indicated the *β* configuration for xylopyranosyl (d, *J* = 7.5 Hz) unit, glucopyranosyl (d, *J* = 7.5/8.0 Hz) unit, and *α* configuration for rhamnopyranosyl (br s) unit. The HMBC correlations from H-1′ (δ_H 4.93) to C-3 (δ_C 89.2) and from H-1′′ (δ_H 5.11) to C-20 (δ_C 83.8) determined the *β*-D-glucose units located at C-3 and C-20, respectively. Similarly, the sugar moiety of C-20 was determined to be *β*-D-xylopyranosyl-(1→3)-*α*-L-rhamnopyranosyl-(1→6)-*β*-D-glucopyranosyl based on the HMBC correlations from H-1′′′′ (δ_H 5.24) to C-3′′′ (δ_C 83.7), H-1′′′ (δ_H 5.42) to C-6′′ (δ_C 68.3) (Fig. 2). The *α* configuration of H-3, H-12, CH_3-21 were substantiated by NOESY correlations of H-3/H-5/H_3-28, H-12/H-17/H_3-30, and H_3-21/H-17 (Fig. 3). The ^{13}C NMR spectral data of the characteristic peaks between the 20(*S*) and 20(*R*) ginsenosides provided information for the identification of the stereoisomers. In particular, changes in the chemical shifts between the *S*- and *R*- forms at C-17, C-21 and C-22 in the ^{13}C NMR spectra were approximately $\Delta\delta$ ($\delta_S - \delta_R$) + 4.1 ± 0.1, + 4.3 ± 0.1, and −7.4 ± 0.1 ppm, respectively [12]. The chemical shifts of C-17 (δ_C 51.8), C-21 (δ_C 22.4), and C-22 (δ_C 36.5) were basically consistent with those of gypenoside XLV [13], thereby the absolute configuration of C-20 was assigned as *S*-form. Therefore, compound **1** was elucidated as (3*β*, 12*β*, 20*S*)-trihydroxydammarane-24-ene-3-*O*-*β*-D-glucopyranosyl-20-*O*-*β*-D-xylopyranosyl-(1→3)-*α*-L-rhamnopyranosyl-(1→6)-*β*-D-glucopyranoside, and named as gypenoside LXXXVIII.

Compound **2**, a white amorphous powder with $[\alpha]_D^{20}$ −33.0 (*c* 0.11, MeOH), had a molecular formula of $C_{59}H_{98}O_{26}$ based on a HRESIMS ion at *m/z* 1221.6276 $[M - H]^-$ (calcd 1221.6268), suggesting 11 degrees of unsaturation. The IR absorptions at 3397 and 1659 cm^{-1} suggested the same functionalities as **1**. The ^1H and ^{13}C NMR data demonstrated that the basic framework of **2** was similar to notoginsenoside-Ng3 [13], Furthermore, the key differences between **1** and **2** were C-12 (δ_{C1} 70.5; δ_{C2} 80.1) and C-23 (δ_{C1} 23.3; δ_{C2} 72.7), which were further authenticated by the HMBC correlations (Fig. 2) from H-12 (δ_H 3.67) to C-23 (δ_C 72.7). In conclusion, these is an ether linkage between C-12 and C-23. The NOESY correlations (Fig. 3) of **2** from H_3-21 to H-13 and H-13 to H_3-18 indicated the *β*-oriented CH_3-21. The NOESY correlations from H-3 to H-5/H-28, H-12 to H-9/H-17/H_3-30 and H-23 to H-12/H-17 indicated the *α* orientation of H-3, H-12 and H-23. The absolute configuration of C-20 was determined as *S*-form through the same procedures as **1** [14]. In addition, the acid hydrolysates of **2** gave the D-glucose, L-rhamnose and D-xylose units. The coupling constant of five anomeric protons means that both glucopyranosyl (d, *J* = 7.5 Hz) and xylopyranosyl (d, *J* = 8.0 Hz) were *β* configuration, and rhamnopyranosyl (br s) was *α* configuration. The NMR data of sugar moieties at C-20 was the same as those of **1**. Moreover, the HMBC correlations of H-1′ (δ_H 4.93)/C-3 (δ_C 89.2) and H-1′′ (δ_H 5.35)/C-2′ (δ_C 83.8) demonstrated that the sugar moieties of C-3 was confirmed to be *β*-D-glucopyranosyl-(1→2)-*β*-D-glucopyranosyl, which was identical to those of notoginsenoside I [15]. Therefore, the structure of **2** was elucidated as (3*β*, 20*S*)-dihydroxy-12*β*, 23*R*-epoxydammarane-24-ene-3-*O*-[*β*-D-glucopyranosyl-(1→2)-*β*-D-glucopyranosyl]-20-*O*-*β*-D-xylopyranosyl-(1→3)-*α*-L-rhamnopyranosyl-(1→6)-*β*-D-glucopyranoside, and named as gypenoside LXXXIX.

Compound **3**, a white amorphous powder with $[\alpha]_D^{20}$ −10.6 (*c* 0.11, MeOH), had a molecular formula of $C_{59}H_{100}O_{27}$ based on a HRESIMS ion at *m/z* 1239.6373 $[M - H]^-$ (calcd 1239.6374). The IR absorptions at 3397 and 1659 cm^{-1} suggested the same functionalities as **1**. The ^1H NMR data (Table 1) of aglycone showed a pair of olefinic protons at δ_H 6.22 (1H, m, H-23) and 6.07 (1H, d, *J* = 15.5 Hz, H-24), which take the place of the $\Delta^{24,\ 25}$ olefinic protons at δ_H 5.32 (1H, m, H-24) of **1**. Furthermore, the key differences between **3** and **1** were C-22 (δ_C 40.1), C-23 (δ_C 123.1), C-24 (δ_C 142.7), C-25 (δ_C 70.3), C-26 (δ_C 30.9), and C-27 (δ_C 30.9), which indicated the existence of an OH-25 group and a $\Delta^{23,\ 24}$ olefinic system in **3**. These are further verified by HMBC cross-peaks (Fig. 2) from H-24 to C-23/C-25/C-26, H_3-26 to C-24/C-25/C-27 and H_3-27 to C-24/C-25/C-26. The NOESY correlations (Fig. 3) of H-3/H-5/H_3-28, H-12/H-9/H-17/H_3-30 and H_3-21/H-17 implying the *α* configuration of H-3, H-12 and CH_3-21. The absolute configuration of C-20 was the similar to notoginsenoside Fh_5 [16]. The ^{13}C NMR data revealed 59 carbon signals, of which 30 carbons for aglycone and 29 carbons for sugar moieties. Via comparing and analyzing the spectroscopic data of **2** and **3**, we find they have the same sugar units and connection mode. With the aid of hydrolysis experiments of **3**, the presence of D-glucose, L-rhamnose and D-xylose was established. Therefore, the structure of **3** was characterized as (3*β*, 12*β*, 20*S*, 25)-tetrahydroxydammarane-23-ene-3-*O*-[*β*-D-glucopyranosyl-(1→2)-*β*-D-glucopyranosyl]-20-*O*-*β*-D-xylopyranosyl-(1→3)-*α*-L-rhamnopyranosyl-(1→6)-*β*-D-glucopyranoside, and named as gypenoside XC.

Compound **4**, a white amorphous powder with $[\alpha]_D^{20}$ + 13.6 (*c* 0.12, MeOH), had a molecular formula of $C_{47}H_{80}O_{17}$ by a HRESIMS ion at *m/z* 915.5326 $[M - H]^-$ (calcd 915.5317). The IR absorptions at 3397 and 1659 cm^{-1} suggested the same functionalities as **1**. Compound **4** showed the similar NMR spectroscopic profile (Table 1) to that of **1**, and the key difference was the sugar units at C-3 and C-20. Apart from 30 carbons for the aglycone, compound **4** showed 17 carbons for sugar moieties. Acid hydrolysis of **4** gave D-glucose and D-xylose units. The coupling constant of three anomeric protons means that glucopyranosyl (d, *J* = 7.5/7.5 Hz) was *β* configuration and xylopyranosyl (d, *J* = 6.5 Hz) was *β* configuration. The location of these sugar moieties was determined by HMBC correlations (Fig. 2) of H-1′ (δ_H 4.83)/C-3 (δ_C 89.1), H-1′′ (δ_H 5.35)/C-2′ (δ_C 83.6), H-3′′′ (δ_H 5.18)/C-20 (δ_C 83.7). Moreover, the sugar moieties at C-3 was further confirmed by the sugar signals from gypenoside XV [17]. The sugar moieties at C-20 were in accordance with those of ginsenoside F_2 [18]. The relative configuration of **4** was described as **1** by explanation of the NOESY data (Fig. 3), and the absolute configuration at C-20 was also assigned as *S*-form by comparing with those data of **1**. Consequently, compound **4** was characterized as (3*β*, 12*β*, 20*S*)-trihydroxydammarane-24-ene-3-*O*-[*β*-D-glucopyranosyl-(1→2)-*β*-D-xylopyranosyl]-20-*O*-*β*-D-glucopyranoside, and named as gypenoside XCI.

Compound **5**, a white amorphous power with $[\alpha]_D^{20}$ −25.5 (*c* 0.11, MeOH), had a molecular formula of $C_{59}H_{100}O_{25}$ based on a HRESIMS ion at *m/z* 1231.6431 $[M + Na]^+$ (calcd 1231.6446). The IR absorptions at 3363 and 1597 cm^{-1} suggested the same functionalities as **1**. The difference of aglycone NMR data between **5** and **1** was a lack of the OH-12,

which was supported by the protons and carbons chemical shifts at C-11, C-12 and C-13 (Table 1). Except for sugar moieties at C-20, compound **5** was similar to notoginsenoside I [15]. But the sugar moiety of C-20 was the same as **1**, which was confirmed by all kinds of NMR data. Acid hydrolysis of **5** gave D-glucose, L-rhamnose and D-xylose units. The configuration was confirmed as that of **1**. Therefore, compound **5** was identified as (3*β*, 20*S*)-dihydroxydammarane-24-ene-3-*O*-[*β*-D-glucopyranosyl-(1→2)-*β*-D-glucopyranosyl]-20-*O*-*β*-D-xylopyranosyl-(1→3)-*α*-L-rhamnopyranosyl-(1→6)-*β*-D-glucopyranoside, and named as gypenoside XCII.

Compound **6**, a white amorphous powder with $[\alpha]_D^{20}$ + 11.4 (*c* 0.12, MeOH), had a molecular formula of $C_{50}H_{84}O_{18}$ based on a HRESIMS ion at *m/z* 971.5586 [M - H]$^-$ (calcd 971.5579). The IR absorptions at 3397 and 1642 cm^{-1} suggested the same functionalities as **1**. The NMR spectroscopic data (Table 2) of **6** was semblable to that of **5**, the only difference is that the sugar moiety at C-20, which revealed the presence of the acetoxyl group at 6′′′- hydroxyl of the C-20 glucosyl moiety in **6** with the help of the HMBC cross-peaks (Fig. 2) of H-1′′′ (δ_H 5.01) to C-20 (δ_C 82.7), C$\underline{H}_3$CO (δ_H 2.08) to CH$_3\underline{C}$O (δ_C 171.2) and C-6′′′ (δ_C 65.5). In addition, D-glucose was detected by acid hydrolysis, and the configuration was confirmed as that of **5**. Thus, the structure of **6** was identified as (3*β*, 20*S*)-dihydroxydammarane-24-ene-3-*O*-[*β*-D-glucopyranosyl-(1→2)-*β*-D-glucopyranosyl]-20-*O*-6-*O*-acetyl-*β*-D-glucopyranoside, and named as gypenoside XCIII.

Compound **7**, a white amorphous powder with $[\alpha]_D^{20}$ −1.5 (*c* 0.12, MeOH), had a molecular formula of $C_{61}H_{102}O_{27}$ based on a HRESIMS ion at *m/z* 1265.6541 [M - H]$^-$ (calcd 1265.6530). The IR spectrum suggested the presence of hydroxyl (3398 cm^{-1}), ester bond (1742 cm^{-1}) and olefinic bond (1642 cm^{-1}) functionalities. Compound **7** showed the similar NMR spectroscopic profile (Table 2) to that of **1** (Table 1), and the key difference was the sugar chains at C-3. By further analysis of NMR data, we know the C-3 sugar chains of **7** were similar to **5**, whereas the 6′-hydroxyl of inner glucose moiety at C-3 was replaced with acetoxyl group. This can be confirmed by the HMBC cross-peak (Fig. 2) from C$\underline{H}_3$CO (δ_H 2.03) to CH$_3\underline{C}$O (δ_C 171.2) and C-6′ (δ_C 64.7), to correspond with that of quinquenoside III [19]. In addition, the glycosylation sites were determined based on the HMBC cross-peaks (Fig. 2) from H-1′ (δ_H 4.85)/C-3 (δ_C 89.8), H-1′′ (δ_H 5.36)/C-2′ (δ_C 83.5), H-1′′′ (δ_H 5.10)/C-20 (δ_C 83.8), H-1′′′′ (δ_H 5.42)/C-6′′′ (δ_C 68.3), H-1′′′′′ (δ_H 5.24)/C-3′′′′ (δ_C 83.7). Acid hydrolysis experiment gave D-glucose, L-rhamnose and D-xylose. The configuration was confirmed as that of **1**. Therefore, compound **7** was assigned as (3*β*, 12*β*, 20*S*)-trihydroxydammarane-24-ene-3-*O*-[*β*-D-glucopyranosyl-(1→2)-6-*O*-acetyl-*β*-D-glucopyranosyl]-20-*O*-*β*-D-xylopyranosyl-(1→3)-*α*-L-rhamnopyranosyl-(1→6)-*β*-D-glucopyranoside, and named as gypenoside XCIV.

Compound **8**, a white amorphous powder with $[\alpha]_D^{20}$ −3.0 (*c* 0.11, MeOH), had a molecular formula of $C_{50}H_{84}O_{18}$ consistent with a HRESIMS ion at *m/z* 971.5572 [M - H]$^-$ (calcd 971.5579). Its IR spectrum showed the hydroxyl (3302 cm^{-1}), ester bond (1743 cm^{-1}), and olefinic bond (1653 cm^{-1}). Comparison of the 1D and 2D NMR data of **8** with that of **5** exhibited the same aglycone moiety. Similarly, sugar chain at C-3 and C-20 were extremely similar to **7** and **4**, respectively. This was confirmed by the strong HMBC correlations (Fig. 2) from H-1′′′ (δ_H 5.09) to C-20 (δ_C 82.7), indicating a glucose moiety at C-20. The other HMBC cross-peaks of CH$_3$CO (δ_H 2.06)/C-6′ (δ_C 64.9), H-1′ (δ_H 4.87)/C-3 (δ_C 89.8), and H-1′′ (δ_H 5.37)/ C-2′ (δ_C 83.6) also provided the evidence for the saccharide chain at C-3. The configuration was confirmed as that of **5**. Connecting with acid hydrolysis, compound **8** was identified as (3*β*, 20*S*)-dihydroxydammarane-24-ene-3-*O*-[*β*-D-glucopyranosyl-(1→2)-6-*O*-acetyl-*β*-D-glucopyranosyl]-20-*O*-*β*-D-glucopyranoside, which was named as gypenoside XCV.

Compound **9**, a white amorphous powder with $[\alpha]_D^{20}$ + 12.8 (*c* 0.12, MeOH). The HRESIMS peak at *m/z* 1103.5990 [M - H]$^-$ (calcd 1103.6002), indicated that the molecular formula of **9** was $C_{55}H_{92}O_{22}$. The IR absorptions at 3397, 1729 and 1598 cm^{-1} suggested the same functionalities as **8**. The NMR data (Table 2) of **9** showed considerable similarities to that of **7**, except for the absence of a *β*-glucose unit on the C-3. HMBC correlations (Fig. 2) of H-1′ (δ_H 4.87)/C-3 (δ_C 89.7), C$\underline{H}_3$CO (δ_H 2.02)/C-6′ (δ_C 65.1) authenticated the 6′-hydroxyl of inner glucose moiety at C-3 was replaced with acetoxyl group. The relative configuration of H-3, H-12, CH$_3$-21 and the absolute configuration of C-20 were substantiated as that of **1**. Combined with acid hydrolysis results, compound **9** was characterized as (3*β*, 12*β*, 20*S*)-trihydroxydammarane-24-ene-3-*O*-(6′-*O*-acetyl-*β*-D-glucopyranosyl)-20-*O*-*β*-D-xylopyranosyl-(1→3)-*α*-L-rhamnopyranosyl-(1→6)-*β*-D-glucopyranoside, which was named as gypenoside XCVI.

Compound **10**, a white amorphous powder with $[\alpha]_D^{20}$ + 11.0 (*c* 0.11, MeOH). The HRESIMS peak at *m/z* 793.4714 [M + Na]$^+$ (calcd 793.4714) indicated the molecular formula of **9** as $C_{41}H_{70}O_{13}$. The IR absorptions at 3329 and 1601 cm^{-1} suggested the same functionalities as **1**. The NMR data (Table 2) were analogous to that of **9**, but an additional hydroxyl substituent at C-2, which was verified by chemical shifts of C-1 (δ_C 48.8), C-2 (δ_C 69.2) and C-3 (δ_C 84.1). Compared with **9**, **10** replaced sugar chain at C-3 with OH-3, which was universally in accordance with those of gynosaponin TN-2 [13]. Acid hydrolysis experiment gave D-glucose and L-arabinose. The coupling constant of two anomeric protons implied that glucopyranosyl (d, J = 7.5 Hz) were *β* configuration and arabinopyranosyl (d, J = 6.0 Hz) was *α* configuration. Moreover, the HMBC correlations (Fig. 2) of H-1′ (δ_H 5.10)/C-20 (δ_C 83.9), H-1′′ (δ_H 4.98)/C-6′ (δ_C 69.7) demonstrated that the sugar moiety of C-20 was confirmed to be *α*-L-arabinopyranosyl-(1→6)-*β*-D-glucopyranoside, corresponding with those of ginsenoside Rb$_2$ [20]. The configuration was confirmed as that of **1**. In conclusion, compound **10** was established as (2*α*, 3*β*, 12*β*, 20*S*)-tetrahydroxydammarane-24-ene-20-*O*-*α*-L-arabinopyranosyl-(1→6)-*β*-D-glucopyranoside, which was named as gypenoside XCVII.

Compound **11**, a white amorphous powder with $[\alpha]_D^{20}$ −24.7 (*c* 0.1, MeOH). The HRESIMS peak at *m/z* 1239.6368 [M - H]$^-$ (calcd 1239.6374) revealed the molecular formula of **11** to be $C_{59}H_{100}O_{27}$. The IR spectrum showed the same functionalities as **1**. Compound **11** showed the similar NMR signals (Table 3) as **1** in terms of aglycone, wheras different chemical shifts of C-25 (δ_C 136.6), C-26 (δ_C 68.4) and C-27 (δ_C 14.4) strongly suggested that the 26-methyl group in **1** was substituted for a methanol group in **11** (Table. 1). This structure of aglycone was corroborated by analogy of the NMR data of gypenoside XVIII [17]. The type of sugar saccharides were established by the acid hydrolysis experiment, and the saccharide sequences and linkage sites were supportive of 2D NMR, which revealed basical similarities to those of **2**. The configuration was confirmed as that of **1**. In summary, compound **11** was elucidated as (3*β*, 12*β*, 20*S*, 26)-tetrahydroxydammarane-24-ene-3-*O*-[*β*-D-glucopyranosyl-(1→2)-*β*-D-glucopyranosyl]-20-*O*-*β*-D-xylopyranosyl-(1→3)-*α*-L-rhamnopyranosyl-(1→6)-*β*-D-glucopyranoside, and termed as gypenoside XCVIII.

Compound **12**, a white amorphous powder with $[\alpha]_D^{20}$ −7.6 (*c* 0.11, MeOH). The molecular formula of **12** was deduced as $C_{47}H_{80}O_{17}$ from the HRESIMS peak at *m/z* 939.5311 [M + Na]$^+$ (calcd 939.5288). The IR spectrum showed the same functionalities as **1**. The saccharide chain at C-20 of **12** was similar to that of **3** on the basis of the ^{1}H and ^{13}C NMR spectra and acid hydrolysis experiment, except for the C-17 chain. The ^{1}H and ^{13}C spectroscopic data (Table 3) showed diagnostic resonances for a pair of olefinic [δ_H 5.26 (1H, s), 4.93 (1H, overlapped); δ_C 110.7] and a methyl group [δ_H 1.96 (3H, s); δ_C 18.5], indicating the presence of a $\Delta^{25,\ 26}$ olefinic system, which was confirmed by HMBC correlations from H$_3$-27 (δ_H 1.96) to C-25 (δ_C 149.9) and C-26 (δ_C 110.7). The hydroxyl substituent was determined by HMBC correlations (Fig. 2), in which cross-peaks were observed from H$_3$-26 (δ_H 5.26 and 4.93) and H$_3$-27 (δ_H 1.96) to a signal at C-24 (δ_C 76.4). By comparing the NMR data of C-20 to C-27 for **12** showed obviously similar signals to those of notoginsenoside LK$_7$ [21]. Finally, compound **12** was deduced as (3*β*, 12*β*,

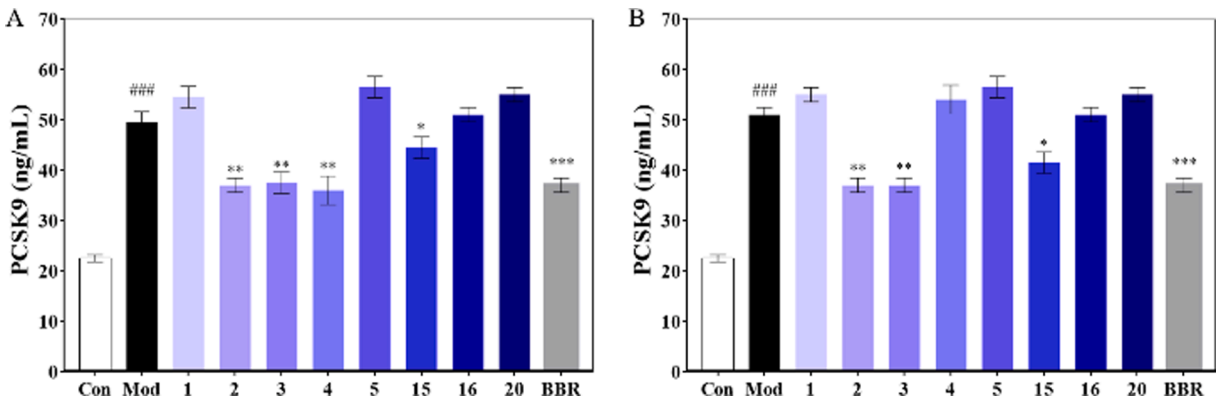

Fig. 4. (A) Effect of compounds from *G. pentaphyllum* on the expression of PCSK9 in HepG2 cells at 20 μM ($^{###}p < 0.001$ vs blank group; $^{*}p < 0.05$, $^{**}p < 0.01$, $^{***}p < 0.001$ vs model group). (B) Effect of compounds from *G. pentaphyllum* on the expression of PCSK9 in HepG2 cells at 10 μM ($^{###}p < 0.001$ vs blank group; $^{*}p < 0.05$, $^{**}p < 0.01$, $^{***}p < 0.001$ vs model group).

20*S*, 24*R*)-tetrahydroxydammarane-25-ene-20-*O*-*β*-D-xylopyranosyl-(1→3)-*α*-L-rhamnopyranosyl-(1→6)-*β*-D-glucopyranoside, and named as gypenoside XCIX.

Compound **13**, a white amorphous powder with $[\alpha]_D^{20}$ −13.0 (*c* 0.11, MeOH). The HRESIMS peak at *m/z* 939.5304 $[M + Na]^+$ (calcd 939.5293), indicated that the molecular formula of **12** was $C_{47}H_{80}O_{17}$. The IR spectrum showed the same functionalities as **1**. Comparation of NMR data (Table 3) of **12** and **13** had nearly the same saccharide chain and basic skeleton but a subtle difference in signals for C-22 (δ_H 2.46/2.18 and δ_C 33.0 in **13**; δ_H 2.59/1.94 and δ_C 33.0 in **12**), C-24 (δ_H 4.46 (dd, 4.5, 7.5) and δ_C 76.4 in **13**; δ_H 4.47 (t, 6,0) and δ_C 76.4 in **12**), and C-26 (δ_H 5.23 (s)/4.89 and δ_C 110.6 in **13**; δ_H 5.26 (s)/4.93 and δ_C 110.7 in **12**). In addition, these compounds differed in the optical rotation, which established the 24(*S*) configuration. Consequently, compound **13** was elucidated as (3*β*, 12*β*, 20*S*, 24*S*)-tetrahydroxydammarane-25-ene-20-*O*-*β*-D-xylopyranosyl-(1→3)-*α*-L-rhamnopyranosyl-(1→6)-*β*-D-glucopyranoside, which termed as gypenoside C.

Compound **14**, a white amorphous powder with $[\alpha]_D^{20}$ + 3.8 (*c* 0.12, MeOH). The molecular formula of **14** was established as $C_{59}H_{100}O_{27}$ by the HRESIMS peak at *m/z* 1239.6381 $[M - H]^-$ (calcd 1239.6374). The IR spectrum showed the same functionalities as **1**. By analyzing NMR data of **14** (Table 3), the basic framework was similar as that of **12**, while the sugar moieties were corresponded with that of **2**. Thus, the structure of **14** was elucidated as (3*β*, 12*β*, 20*S*, 24*R*)-tetrahydroxydammarane-25-ene-3-*O*-[*β*-D-glucopyranosyl-(1→2)-*β*-D-glucopyranosyl]-20-*O*-*β*-D-xylopyranosyl-(1→3)-*α*-L-rhamnopyranosyl-(1→6)-*β*-D-glucopyranoside, which named as gypenoside CI.

The isolated six known compounds (**15**–**20**) were identified as ginsenoside Rg_5 (**15**) [22], ginsenoside Rg_3 (**16**) [23], ginsenoside F_2 (**17**) [24], gypenoside LI (**18**), gypenoside L (**19**) [25], gypenoside XIV (**20**) [18] by comparison of the spectroscopic data with those reported in the literature.

Inhibiting PCSK9 to enhance the effect of statins provides another treatment option for patients who need to further reduce LDL-C. At present, PCSK9 monoclonal antibodies have been showed satisfied clinical benefits. However, high cost and inconvenient subcutaneous administration have resulted in the need for low-cost and oral chemicals to regulate PCSK9 [26]. Due to various health-promoting functions, *G. pentaphyllum* have been consumed as a kind of functional tea beverage in China for a long time [6]. However, more knowledge on the profile and PCSK9 inhibitory activity of phytochemicals is needed to better understand the beneficial effects of the plant. In this study, eight isolates were evaluated the inhibitory effect on PCSK9 in HepG2 cells, and berberine (10 μM) was selected as positive control. The results showed that four dammarane-type glycosides (**2**–**4**, **15**) remarkably reduced PCSK9 expression at 20 μM concentration (Fig. 4A). Especially, compounds **2**, **3** and **15** exhibited significant inhibitory effect on PCSK9 expression at 10 μM concentration compared to the control (Fig. 4B).

Triterpene saponins have been shown to possess a wide range of biological activities. In this study, we determined the antilipidemic activity of these compounds, eight isolates were evaluated the inhibitory effect on PCSK9 in HepG2 cells. Compounds **1**, **5**, **16** and **20** did not show significant inhibitory effects on PCSK9 in HepG2 cells (Fig. 4A), which might be due to its structure that makes it difficult for these compounds bind to the PCSK9 protein. However, three dammarane-type glycosides (**2**, **3**, **15**) remarkably reduced PCSK9 expression at 10 μM concentration, in which compound **2** possess a unusual cyclization and compounds **3**, **15** possess carbon–carbon double bond at C-23 and C-20 respectively, it may be the active group for its inhibitory effects on PCSK9.

However, these are still some limitations in this study, such as limited number of monomer compounds screened, lack of structural diversity, small number of samples and only cell level screening. Therefore, the chemical constituents of *G. pentaphyllum* from Guangxi resource can be further separated and enriched, and the structure–activity relationship can be further explored. Finally, the compounds with good cellular activity can be verified in animal models.

4. Conclusion

Taken together, in this study, we isolated 20 triterpene saponins, including fourteen novel ones from *G. pentaphyllum*. The inhibitory effects on PCSK9 of these compounds were determined in HepG2 cells. Three dammarane-type glycosides (**2**, **3**, **15**) remarkably reduced PCSK9 expression at 10 μM concentration. These findings suggested that *G. pentaphyllum* was worthy of further investigation to find small molecule PCSK9 inhibitors and facilitate their utilization of the plant materials as hyperlipidemia preventive agents.

Declaration of Competing Interest

The authors declare that they have no known competing financial interests or personal relationships that could have appeared to influence the work reported in this paper.

Acknowledgements

This work was financially supported by National Key Research and Development Project (No. 2019YFC1711000), Scientific Research Innovation Program of Jiangsu Graduate (No. KYCX20_0676), Qing Lan Project of Jiangsu Higher Education Institutions and the Funding of Double First-rate Discipline Innovation Team [CPU2018GF05, CPU2018GY31].

Appendix A. Supplementary data

Supplementary data to this article can be found online at https://doi.org/10.1016/j.bioorg.2021.104843.

References

[1] F. Yin, L.H. Hu, F.C. Lou, R.X. Pan, Dammarane-type glycosides from *Gynostemma pentaphyllum*, J. Nat. Prod. 67 (6) (2004) 942–952.

[2] L. Shi, F. Lu, H. Zhao, Y.Q. Zhao, Two new triterpene saponins from *Gynostemma pentaphyllum*, J. Asian Nat. Prod. Res. 14 (9) (2012) 856–861.

[3] K.J. Li, C. Ma, H.Y. Li, S. Dev, J.F. He, X.S. Qu, Medicinal value and potential therapeutic mechanisms of *Gynostemma pentaphyllum* (thunb.) makino and its derivatives: An overview, Curr. Top. Med. Chem. 19 (31) (2019) 2855–2867.

[4] M.J. Yin, J.J. Zhang, L.Z. Wang, F.Y. Li, Z.F. Li, W. Xiang, S.T. Bie, C.H. Wang, Z. Li, Ten new dammarane-type saponins with hypolipidemia activity from a functional herbal tea-*Gynostemma pentaphyllum*, Molecules 25 (16) (2020) 3737.

[5] Y.G. Niu, W. Yan, J.L. Lv, W.B. Yao, L.L. Yu, Characterization of a novel polysaccharide from tetraploid *Gynostemma pentaphyllum* makino, J. Agric. Food Chem. 61 (20) (2013) 4882–4889.

[6] X.Y. Xia, J. Xu, X.D. Wang, H. Wang, Z.C. Lin, K.P. Shao, L.L. Fang, C.N. Zhang, Y. Q. Zhao, Jiaogulan tea (*Gynostemma pentaphyllum*) potentiates the antidiabetic effect of white tea via the AMPK and PI3K pathways in C57BL/6 mice, Food. Funct. 11 (5) (2020) 4339–4355.

[7] M.G. Silverman, B.A. Ference, K. Im, S.D. Wiviott, R.P. Giugliano, S.M. Grundy, E. Braunwald, M.S. Sabatine, Association between lowering LDL-C and cardiovascular risk reduction among different therapeutic interventions: a systematic review and meta-analysis, J. Am. Med. Assoc. 316 (12) (2016) 1289–1297.

[8] F. Mach, C. Baigent, A.L. Catapano, K.C. Koskinas, M. Casula, L. Badimon, M.J. Chapman, G.G. De Backer, V. Delgado, B.A. Ference, I.M. Graham, A. Halliday, U. Landmesser, B. Mihaylova, T.R. Pedersen, G. Riccardi, D.J. Richter, M.S. Sabatine, M.R. Taskinen, L. Tokgozoglu, O. Wiklund, ESCSD. Group, 2019 ESC/EAS guidelines for the management of dyslipidaemias: lipid modification to reduce cardiovascular risk, Eur. Heart. J. 41 (1) (2020) 111–188.

[9] N.Y. He, Q. Li, C.Y. Wu, Z. Ren, Y. Gao, L.H. Pan, M.M. Wang, H.Y. Wen, Z.S. Jiang, Z.H. Tang, L.S. Liu, Lowering serum lipids via PCSK9-targeting drugs: current advances and future perspectives, Acta. Pharmacol. Sin. 38 (3) (2017) 301–311.

[10] L.S. Wu, M.Z. Qian, Effects of gypenosides on PCSK9 gene expression and blood lipids lowered by simvastatin, Chin. J. Pathophysiol. 33 (1) (2017) 79–85.

[11] T. Tanaka, T. Nakashima, T. Ueda, K. Tomii, I. Kouno, Facile discrimination of aldose enantiomers by reversed-phase HPLC, Chem. Pharm. Bull. (Tokyo) 55 (6) (2007) 899–901.

[12] H. Yang, J.Y. Kim, S.O. Kim, Y.H. Yoo, S.H. Sung, Complete ^{1}H-NMR and ^{13}C-NMR spectral analysis of the pairs of 20(*S*) and 20(*R*) ginsenosides, J Ginseng Res. 38 (3) (2014) 194–202.

[13] T. Takemoto, S. Arihara, K. Yoshikawa, J. Kawasaki, T. Nakajima, M. Okuhira, Studies on the constituents of cucurbitaceae plants. XI. on the saponin constituents of *Gynostemma pentaphyllum* makino (7), Yakugaku Zasshi 104 (10) (1984) 1043–1049.

[14] J.W. Huang, C.J. Li, J.Z. Cao, J. Ma, Y.Q. Du, X.Y. Liu, J.Z. Yang, D.M. Zhang, New dammarane-type saponins from the leaves of *Panax notoginseng*, Chin. Chem. Lett. 30 (2) (2019) 447–450.

[15] M. Yoshikawa, T. Murakami, T. Ueno, N. Hirokawa, K. Yashiro, N. Murakami, J. Yamahara, H. Matsuda, R. Saijoh, O. Tanaka, Bioactive saponins and glycosides. IX. notoginseng (2): structures of five new dammarane-type triterpene oligoglycosides, notoginsenosides-E, -G, -H, -I, and -J, and a novel acetylenic fatty acid glycoside, notoginsenic acid β-sophoroside, from the dried root of *Panax notoginseng* (BURK.) F. H. Chen, Chem. Pharm. Bull. (Tokyo) 45 (6) (1997) 1056–1062.

[16] X.Y. Liu, S. Wang, C.J. Li, J. Ma, F.Y. Chen, Y. Peng, X.L. Wang, D.M. Zhang, Dammarane-type saponins from the leaves of *Panax notoginseng* and their neuroprotective effects on damaged SH-SY5Y cells, Phytochemistry 145 (2018) 10–17.

[17] T. Takemoto, S. Arihara, T. Nakajima, M. Okuhira, Studies on the constituents of *Gynostemma pentaphyllum* makino. II. structures of gypenoside XV-XXI, Yakugaku Zasshi 103 (10) (1983) 1015–1023.

[18] T. Takemoto, S. Arihara, T. Nakajima, M. Okuhira, Studies on the constituents of *Gynostemma pentaphyllum* makino. I. structures of gypenoside I-XIV, Yakugaku Zasshi 103 (2) (1983) 173–185.

[19] M. Yoshikawa, T. Murakami, K. Yashiro, J. Yamahara, H. Matsuda, R. Saijoh, O. Tanaka, Bioactive saponins and glycosides. XI. structures of new dammarane-type triterpene oligoglycosides, quinquenosides I, II, III, IV, and V, from American ginseng, the roots of *Panax quinquefolium* L, Chem. Pharm. Bull. (Tokyo) 46 (4) (1998) 647–654.

[20] Y.J. Sun, H. Chen, Z.Y. Hao, J.M. Wang, Y.L. Zhang, X. Zhao, Y.N. Zheng, Chemical constituents from fruit of *Panax ginseng*, J. Chin. Med. Mater. 37 (8) (2014) 1387–1390.

[21] J. Li, R.F. Wang, Y. Zhou, H.J. Hu, Y.B. Yang, L. Yang, Z.T. Wang, Dammarane-type triterpene oligoglycosides from the leaves and stems of *Panax notoginseng* and their antiinflammatory activities, J Ginseng Res. 43 (3) (2019) 377–384.

[22] J. Meng, W.W. Duan, Minor triterpene saponins from the leaves of *Panax ginseng*, West China. J. Pharm. Sci. 32 (3) (2017) 284–286.

[23] L.Q. Cheng, J.R. Na, M.H. Bang, M.K. Kim, D.C. Yang, Conversion of major ginsenoside Rb_1 to 20(*S*)-ginsenoside Rg_3 by *Microbacterium* sp. GS514, Phytochemistry 69 (1) (2008) 218–224.

[24] L.Q. Cheng, M.K. Kim, J.W. Lee, Y.J. Lee, D.C. Yang, Conversion of major ginsenoside Rb_1 to ginsenoside F_2 by *Caulobacter leidyia*, Biotechnol. Lett. 28 (14) (2006) 1121–1127.

[25] T. Takemoto, S. Arihara, K. Yoshikawa, K. Hino, T. Nakajima, M. Okuhira, Studies on the constituents of cucurbitaceae plants. XII. on the saponin constituents of *Gynostemma pentaphyllum* makino (8), Yakugaku Zasshi 104 (11) (1984) 1155–1162.

[26] T. Nishikido, K.K. Ray, Non-antibody approaches to proprotein convertase subtilisin kexin 9 inhibition: siRNA, antisense oligonucleotides, adnectins, vaccination, and new attempts at small-molecule inhibitors based on new discoveries, Front. Cardiovasc. Med. 5 (2018) 199.